Article

The Effects of Atmospheric Attenuation on Cosmic Ray Muons: How is Surface Level Cosmic Ray Muon Flux Affected by Atmospheric Attenuation?

[1]Daniel Sun, [2]Dr. Steve Sun, [1]Michael O'Byrne
[1]Interlake High School, Bellevue, Washington
[2]Independent Researcher, Redmond, Washington

SUMMARY

Cosmic rays are high-energy astronomical particles originating from various sources across the universe. After undergoing nuclear reactions in the upper atmosphere, the primary form they take on the Earth's surface is in the form of muons. Here, we sought to understand how surface-level cosmic-ray muon flux is affected by atmospheric attenuation by measuring the variation in relative muon-flux rate relative to zenith angle, testing the hypothesis that muons follow an exponential attenuation model. Using a QuarkNet cosmic ray muon detector (CRMD), we collected relative muon-flux data while varying the rotational orientation of the CRMD with respect to the magnetic east-west axis. We then calculated a sensitivity function for the detector with respect to muon entry angle. We parameterized a relative muon angular-density function based on the model of exponential attenuation through the Earth's atmosphere. Then, we convolved these functions and fitted parameters to experimental data using least-squares regression. The attenuation model predicts an attenuation length of 6.3 km. This result implies that only a maximum of 24% of muons can reach the Earth's surface, due to both decay and atmospheric interactions. The agreement between data and model ($\chi^2=0.351$) provides evidence of exponential muon attenuation through the atmosphere.

INTRODUCTION

Cosmic rays are high-energy, astronomical particles that can strike the Earth from space. Typical primary cosmic rays are composed of about 90% protons, 9% alpha particles, and 1% high atomic number and energy (HZE) ions. Most cosmic rays are accelerated in the shock waves of supernova remnants (1). Cosmic rays can also be generated by colliding galaxies and active galactic nuclei (2).

Cosmic rays are among the most energetic particles found on Earth. The most energetic among them can have $\sim 10^6$ times more energy than the most energetic protons generated in today's particle accelerators (3). While average cosmic rays are several orders of magnitude less energetic, typically around 1 gigaelectronvolt (GeV), they are still energetic enough to cause nuclear chain reactions in the upper atmosphere known as air showers (4, 5).

Muons are formed in secondary decay processes from primary cosmic rays as well as in tertiary and further decay processes from other energetic decay products. They constitute a significant proportion of air showers. Since they are leptons, they do not interact with the strong force (6). These characteristics, and their very high speed, explain muons' high penetration capabilities: they can penetrate through the Earth's atmosphere and up to a few kilometers of solid rock (7). However, despite having a high penetration depth, muons are still significantly attenuated by the Earth's atmosphere.

Muons are charged elementary leptons in the second generation of the Standard Model, with about 200 times the rest mass of an electron (8). Muons interact with the electromagnetic force, the weak force, and gravity. The lack of muon strong interaction helps them pass through atomic matter with more ease than particles such as hadrons, which explains why cosmic rays are almost always seen as byproducts of the nuclear reactions they are involved in. Furthermore, the high energy of muons puts them in the realm of special relativity, where effects like time dilation and length contraction help them survive considerably longer than predicted through Newtonian mechanics (9). Further details about the common generation and decay mechanisms of cosmic ray muons can be found in **Appendix A**.

Despite penetrating through significant thicknesses of most materials, muons can be detected by exploiting the fact that they are charged particles. Hence, they can cause certain materials to scintillate. The QuarkNet cosmic ray muon detector (CRMD) exploits this fact to detect muons. It consists of four scintillator plates and their associated photomultiplier tubes (PMTs), a power distribution unit (PDU), a data acquisition board (DAQ), a GPS unit, and bundled EQUIP software.

When an energetic muon passes through a scintillator plate, the plate fluoresces and produces photons. Radiated photons undergo total internal reflection inside the optically insulated plate until they reach the PMT. There, they produce a small photocurrent, which is then amplified by a series of

dynodes through a potential drop of a little less than a kilovolt until it reaches a more easily measurable value. This signal is sent to the DAQ board, where onboard logic processes these signals and sends formatted data via a serial port to a computer for further analysis (10). However, the detector is not perfect – it may report electronic noise as a muon event or fail to report the passing of an undetected muon. For clarity, the flux reported by the CRMD shall henceforth be known as the relative muon flux.

The experiment was designed around the hypothesis that muons follow an exponential attenuation model: muons decay or are otherwise destroyed exponentially with distance travelled through the Earth's atmosphere. One of the major sources of this phenomenon, decay, is exponential in time (and therefore in distance), motivating this study to find if other sources of muon interaction are exponential as well. If they are, then we can succinctly summarize the overall atmospheric effect on muons in an exponential attenuation model. Our regression predicted an attenuation length of 6.3 km. The agreement between data and model ($\chi^2 = 0.351$) supports the hypothesis of exponential muon attenuation through the atmosphere.

RESULTS

Since the area of the scintillator plates remained unchanged throughout the experiment, the number of muons detected per unit time was proportional to the relative muon flux. To find the effect of atmospheric attenuation on muons, we conducted an experiment measuring relative muon flux while varying the scintillator plates' zenith angle. We calculated a relative sensitivity function of muon entry angle relative to the scintillator plates from the scintillator plates' measured geometry. We parameterized a relative muon density function of zenith angle using an exponential attenuation model and atmospheric geometry. We fitted the convolution of the relative sensitivity function and muon density function using least squares regression to relative muon-flux observations. Finally, we analyzed the parameters of the relative muon density function to learn about the atmospheric attenuation of cosmic ray muons.

We collected a large amount of raw data, and for the purposes of clarity, selected summary data tables can be found in **Appendix B**. The highest measured relative muon-flux rate was at $\theta = 0°$ with 348 ± 3.1 min^{-1}, while the lowest measured relative muon-flux rate was at $\theta = 87.2$ with 39.6 ± 0.6 min^{-1} (**Appendix B**, **Table 1**).

With the parameters found from the regression, we gleaned important information regarding muons and their attenuation behavior through the atmosphere. We used the classical attenuation equation as $f(d) = Ae^{-d/\lambda}$, where d is distance travelled through the medium and λ is the attenuation length of the medium. While the parameter $A = 1522$ is only for scaling (**Appendix B**, **Table 2**), it represents the observed angular muon density. The parameter $\alpha = 1015$ appeared in our attenuation equation as $f(\theta) = Ae^{-\alpha d(\theta)/R}$, where

$R = 6371$ km is the radius of the Earth. This reveals that the attenuation length is $\lambda = R/\alpha = 6.3$ km, which is the measured atmospheric attenuation length for typical cosmic ray muons. In other words, about 37% of muons will survive for every interval of 6.3 km. The proportion of head-on muons that survive is $e^{-h/\lambda} = 0.24$, where $h = 9$ km is the approximate height of muon generation, and the proportion of extreme-entry muons that survive is $e^{-d/\lambda} = 2.4 \times 10^{-24}$, where $d = 340$ km is the muon generation height at an angle of $\theta = 90°$. Our fit for the parameters within our model had a high correlation, with a chi-squared test yielding $\chi^2 = 0.351$ (**Figure 1**).

Assuming that the number of incoming muons are proportional to the atmosphere's surface area for any angle, the ratio of muons measured on a point on Earth's surface with atmospheric attenuation effects to the expected muons measured at the same point without atmospheric attenuation effects can be shown to be 3.9×10^{-4}. However, this is purely theoretical, as without the atmosphere, muons would not be generated from cosmic rays in the first place. The details pertaining to this calculation can be found in **Appendix C**.

Magnetic field effects

Muons are charged particles, and they will be impacted by the Earth's magnetic field. Since the height of the apparatus above the ground (~3 meters) is much less than the Earth's radius, we can assume that the most extreme muon entry angle is 90° with respect to the vertical. This extreme trajectory is collinear with the line GO' (**Figure 2**). Solving for d, $d = (2hR + h^2)^{1/2}$. Using $R = 6371$ km and $h = 9$ km, $d \approx 340$ km. This gives $h/R = 9/6371 \approx 0.0014$. For a muon travelling orthogonal to a uniform magnetic field in a circular trajectory, $F = (ymv^2)/R = qvB$. The arclength of the muon trajectory, EO', is $L = R\theta$ (**Figure 3**). Thus $R\theta = vt$. Rearranging, $Rt = (R^2\theta)/v$. From trigonometry, $d = 2Rsin(\theta/2)$. Using the small-angle approximation for $sin\theta$ yields $d \approx R\theta$. Thus, $d \approx L = vt = (qBR)*t/(ym)$. Substituting values for Rt and R and solving for
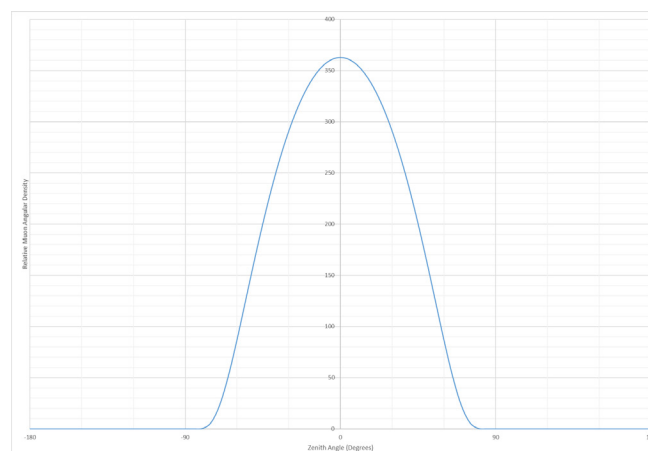
Figure 1. Relative muon angular density vs. zenith angle (degrees). This was the attenuation function produced by the model, plotted using parameters A and α from our regression.
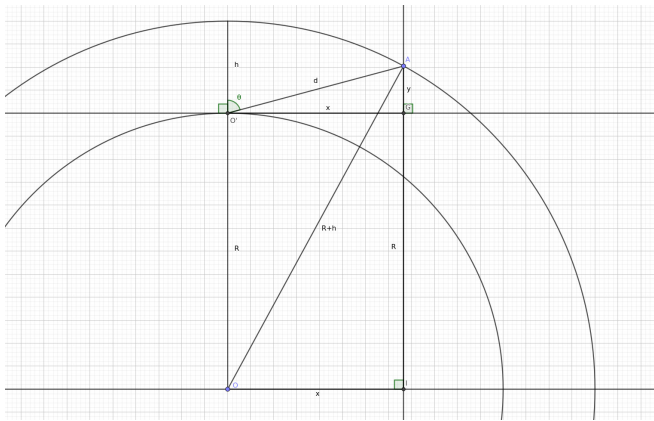
Figure 2. Cross-section of Earth showing arbitrary muon entry angle. The center of the earth is denoted by O, the detector by O', the Earth's surface by the inner circle, and the level where muons are created by the outer circle. d denotes distance travelled by the muon, R denotes the radius of the Earth, and h denotes the height above the Earth's surface at which muons are generated. The path of the muon is denoted by $\overline{AO'}$, where A is where the muon enters.
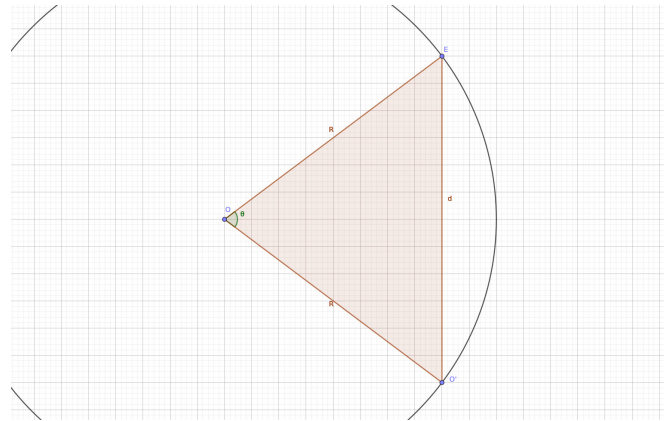

Figure 3. Muon deflection in a uniform magnetic field. O denotes the center of curvature, the arc EO' denotes the trajectory of the muon, E denotes the entry point of the muon, and O' denotes the detector. The uniform magnetic field comes out of the page.

θ yields $\theta \approx (dqB)/(\gamma mv)$. Assuming $B \approx 0.5$ Gauss, for $d = 9$ km, or a muon travelling straight down, deflection is negligible, at roughly 2°. However, at $d \approx 340$ km, deflection is no longer non-negligible, at 70°. However, this issue can be solved. The magnetic field points toward the Earth's magnetic south pole, so any deflection of a muon will be in the direction of magnetic east-west. However, if the detector is rotated along the magnetic east-west axis, then data will be collected on variations in magnetic north-south motion of muons. Since there is no magnetic deflection this way, we avoided the problem of Earth's magnetic field.

Solar effects

The Sun is a minor, almost negligible source of cosmic rays at the energies of interest for the CRMD. However, its solar wind has a significant, non-negligible effect on the Earth's magnetosphere. Since factors stemming from this variation are difficult to model and compute accurately, trials were conducted at roughly the same time of day each day. This ensured relatively good consistency in the state of the magnetosphere among each trial conducted.

DISCUSSION

The high correlation ($\chi^2 = 0.351$) from our theoretical model to experimental data supports the hypothesis of exponential attenuation behavior for cosmic ray muons, with an empirically derived attenuation length of roughly $\lambda = 6.3$ km. This predicts that 24% of "head-on" muons entering the Earth's atmosphere will make it to the surface. This prediction is lower than the 70% survival rate predicted by special relativity and decay only (**Appendix A**). This is likely due to interactions with the atmosphere, such as those that create secondary cosmic ray showers. Since both attenuation and decay are exponential functions of distance, this comparison shows that atmospheric

interactions are the dominant factor in limiting a muon's survivability. Furthermore, the extremely low survivability of muons in extreme-entry angles shows that most muons detected on the ground come from angles close to vertical as supported by the relative muon-flux intensity measured at different angles in this experiment (**Appendix B**, **Table 1**).

The methodology used in this investigation provides an easy and convenient way to perform studies with increased atmospheric depth without the need for physically elevating the detector. The convolution method presented allows rough measurements with the detector to be deconvolved to an angular distribution associated with an atmospheric depth greater than the local vertical atmospheric depth. For this experiment, the calculated attenuation length likely includes effects from muon decay, atmospheric effects, and other effects. At this point, it is an empirical value, as are most attenuation lengths in the current literature (11, 12).

Errors in the experiment may have stemmed from the construction of the device itself, as evidenced by the need for a plateauing process, as the PMTs all have different optimal operating voltages. Although the execution of a plateauing process lessened these inconsistencies, they still existed to some extent. Compounding this issue was the prevalence of false positives and false negatives in the detector. Further sources of error arose from the 0.5° resolution of the protractor we used to measure the detector angle and the measurement uncertainty of the detector's dimensions used in constructing a mathematical model for the detector.

Additionally, one of our assumptions was that muon events are random and independent and follow a Poisson distribution. However, the mechanism for producing muons creates jets of multiple closely spaced muons, so the actual distribution of muons may not be perfectly Poisson. The influence of such errors may merit further study.

For further research into this subject, the resolution of the changes in angle could be refined to 0.5°, which is equivalent

to the resolution of the protractor used in this experiment. The number of events observed could be increased to at least 40,000 to reduce the Poisson relative uncertainty of the count of muon events within a particular timeframe to at most 0.5%. Moreover, the number of PMTs used can be increased to four to reduce false positives in the coincidence data, though this could come at the cost of introducing more false negatives. Continuous convolution could be used instead of discrete convolution to obtain a more mathematically accurate result. A more versatile frame for the boards can be constructed to allow the spacing between the boards to be varied to confirm the model developed in this experiment more clearly. Additional research can be conducted with increasingly complex attenuation models, considering the varying density, pressure, and temperature of Earth's atmosphere as well as characteristics of Earth's magnetic field. The methodology developed in this experiment is versatile for conducting experiments about varying atmospheric depth and could be used for further related research.

MATERIALS AND METHODS
Apparatus
The cosmic ray muon detector (CRMD) is comprised of multiple components working in tandem, coordinated by the data acquisition (DAQ) board. Overall, the system consists of the DAQ board, the scintillator plates, the photomultiplier tubes (PMTs), the power distribution unit (PDU), the global positioning system (GPS) unit, and the computer. The scintillator plates and PMTs were pre-assembled into a rigid wooden frame with a flat base (**Figure 4**).

Scintillator plates and PMTs
The scintillator plates in the CRMD are made of plastic wrapped in foil. These plates are then joined to the PMT with

Figure 4. The CRMD in operation. Visible are the scintillator plates and PMTs stacked in a wooden frame. The angle the base of the frame makes with the floor was measured as the independent variable. The DAQ and PDU (not pictured) were placed behind the frame.

an optical cookie, and the entire assembly is wrapped in light insulation (10). When a muon passes through the scintillator plate, the PMT assembly sends a current to the DAQ board. The PMTs have a total voltage drop of around a kilovolt, supplied by the PDU, which generates PMT amplification.

PDU
The PDU receives its power from the DAQ board and can supply precise voltage to the PMTs. The PDU is used for fine-tuning the voltage of the PMTs to set up their sensitivity, a vital step known as plateauing the PMT sensitivity. This step reduces both the chance of noise contamination and missing the detection of a muon. More about this process can be found in **Appendix D**.

DAQ board
The DAQ board applies several selection criteria to determine whether the signals it receives from the PMTs constitute the same muon event, known as coincidence. Generally, if signals from the PMT occur within a specified time window (300 nanoseconds), they are treated as having been caused by the same muon. If only a board or two are triggered, the DAQ registers the event as dark noise and the measurement is not recorded.

GPS
The time-based calculations made by the DAQ board are possible due to a fast onboard clock, ticking once per 1.25 nanoseconds. This clock is periodically synchronized with the clock from the GPS unit to correct small drifts in timing. The GPS unit also provides information about latitude, longitude, and elevation, which can be important in determining the effect of the Earth's magnetic field on the muons and local muon flux, as many different factors can affect muon flux across the world. Due to poor GPS design, the firmware needed to be updated to correctly synchronize the clock. Details about the update process can be found in **Appendix E**.

EQUIP
The experiment is controlled through the EQUIP application's terminal emulator and graphical user interface (GUI). We used EQUIP to configure data output and DAQ onboard logic through a serial port connection to the DAQ board. We adjusted the DAQ settings such that the data stream from the DAQ was saved into a text file for further analysis (9). EQUIP settings can be found in **Appendix F**.

Rotation
For reasons previously discussed, the plate apparatus was rotated along the magnetic east-west axis. The apparatus was rotated by putting a stack of books under the frame (**Figure 4**). A step size of 5° was chosen to be appropriate for this method of rotation. The angle that the base of the apparatus made with the floor was then measured with a standard protractor. This setup was exceptionally stable and provided a standard

for consistent data collection.

Mathematical Model
Relative detector sensitivity function

The sensitivity function of the detector gives the relative probability that a muon will be detected in terms of its angle θ relative to the normal axis of the scintillator plates and in the plane of the axis of rotation of the detector. Since the length of the plates along the long axis was along the axis of rotation, it is constant for all detector orientations in this experiment and angles of muon entry. It is only necessary to consider the two-dimensional angle in the following analysis.

Assuming that muons are generated at random in general, all muon events measured by the CRMD are essentially independently and randomly distributed. Therefore, we modeled the relative muon flux detected by the CRMD in each time interval as a Poisson distribution (13). We assume that muons cannot pass through the Earth, and that the Earth is a perfect sphere.

Muons are equally distributed across space for a given angle. We assumed that the probability of a detection event is directly proportional to the probability that a muon passes through all four boards. If a muon passes through the two boards on both ends, then it must also pass through the two boards in the middle.

Consider the two outermost rectangular faces. The probability that a muon is detected, given an angle, is proportional to the valid area of capture. Since the plates' length is a constant, the probability is proportional to the width of capture. The muons enter the detector on lines parallel to $\overline{GD}$ and $\overline{BF}$ (**Figure 5**). These lines represent the extreme locations where the muon will still pass through both plates, and therefore have a chance at being detected. Solving for lengths, $AE = h \tan \theta$, $BE = w - h \tan \theta$, and $x = BE \cos \theta = w \cos \theta - h \sin \theta$ for $0 \leq \theta \leq \pi/4$.

According to our model, perpendicular muons have capture width w. If a perpendicular muon is considered to have unitary probability, since the probability function is relative, the sensitivity function takes the form $g(\theta) = (w \cos \theta - h \sin \theta)/w$ for $0 \leq \theta \leq \pi/4$. Measurements of the scintillator plates reveal $w = 26$ cm and $h = 26$ cm, so the calculated sensitivity function is $g(\theta) = \cos \theta - \sin \theta$ for $0 < \theta < \pi/4$. The full definition, considering signage, across the domain $-7\pi/4 \leq \theta \leq 7\pi/4$ is (**Figure 6**):

$$g(\theta) = \begin{cases} -\cos\theta - \sin|\theta + \pi|, & -\dfrac{5\pi}{4} \leq \theta \leq -\dfrac{3\pi}{4} \\ \cos\theta - \sin|\theta|, & \dfrac{\pi}{4} \leq \theta \leq \dfrac{\pi}{4} \\ -\cos\theta - \sin|\theta - \pi|, & \dfrac{3\pi}{4} \leq \theta \leq \dfrac{5\pi}{4} \\ 0, & otherwise \end{cases} \quad (1)$$

Discrete convolution

Convolution is defined as $(f * g)(\theta) = \int_{-\infty}^{\infty} f(\varphi)g(\theta - \varphi)d\varphi$. Here, $f(\theta)$ refers to relative muon angular density and $g(\theta)$ is defined above. Since $g(\theta)$ is an even function and $f(\theta)$ has domain $-\pi \leq 0 \leq \pi$, setting proper integration limits yields $(f * g) = \int_{-\pi}^{\pi} f(\varphi)g(\varphi - \theta)d\varphi$. For each angle φ, $f(\varphi)g(\varphi - \theta)$ gives the density of observed muons. Integrating this over the range of all angles yields relative muon flux. θ expresses the rotation of the detector as a linear translation of the sensitivity curve in angular space. The magnitude of θ will not exceed $3\pi/4$ because of the design of the detector. This lets us restrict the
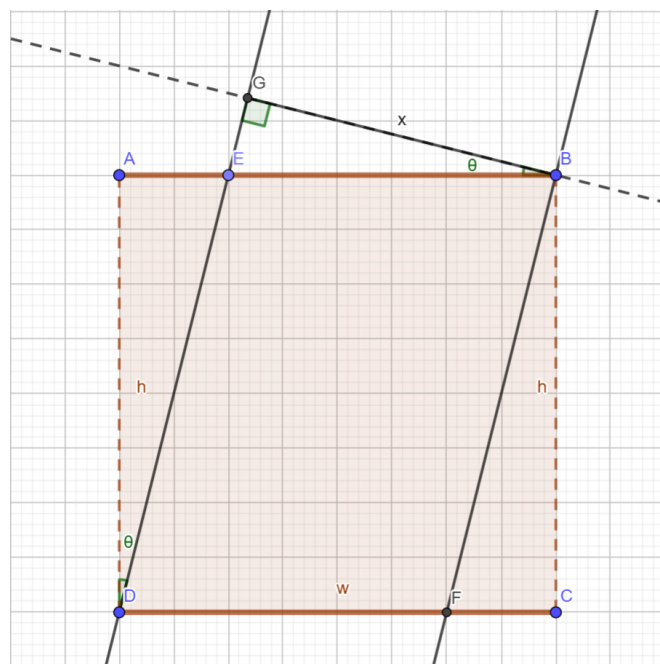
Figure 5. Side view of top and bottom faces of the scintillator plates. Muons enter along the two parallel black lines. The axis of rotation goes into the page. x denotes the width of capture, w represents the width of the plate along the short axis, h represents the separation between the top face of the top plate and bottom face of the bottom plate, and θ represents muon angle relative to the vertical.
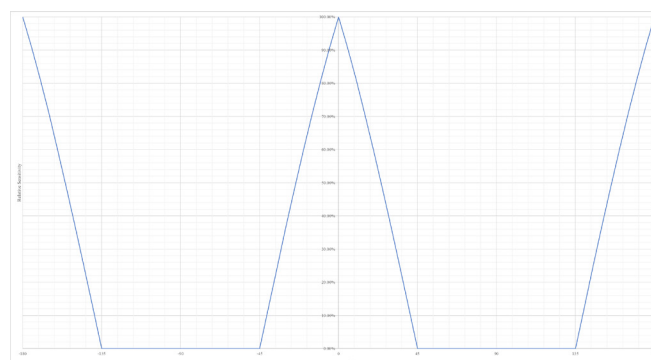
Figure 6. Relative detector sensitivity vs. muon angle (degrees). Equation 1 is plotted. Muon angle was taken relative to the axis of the detector. The range from -180° to 180° is illustrated to account for the fact that muons can enter from both sides of the detector.

domain for the sensitivity function to $7\pi/4 \le \theta \le 7\pi/4$.

However, due to the characteristics of this experiment, it is improper to integrate these functions, considering them as continuous. Data collected regarding angle is discrete. The resolution used for this experiment was $5° = \pi/36$. In addition, a normalization factor was added to the convolution to account for the fact that $g(\theta)$ is unnormalized. Let $\mu g = \Sigma^9_{i=-9} g(i\pi/36)$. Then the discrete convolution is defined:

$$(f * g)(\theta) = \frac{1}{\mu_g} \sum_{i=-36}^{36} f\left(\frac{\pi}{36}i\right) g\left(\frac{\pi}{36}i - \theta\right) \quad (2)$$

The step size required for this discrete convolution step necessitated interpolation of the data, which added a source of random error to the experiment.

Zenith angle and atmospheric depth

Zenith angle, or the angle from the normal of the scintillator plates to the zenith on the Earth's surface, is related to the atmospheric depth that the muons travel through to reach the detector (**Figure 2**).

From the definition of a circle, $x^2 + (y + R)^2 = (R + h)^2$. Substituting $x^2 + y^2 = d^2$ and $y = d \cos \theta$ reveals a quadratic in d, $d^2 + 2R \cos \theta\, d - 2hR - h^2 = 0$, which can be solved to yield:

Procedure

$$d = R\left(-\cos\theta + \sqrt{\cos^2\theta + \left(\frac{h}{R}\right)^2 + \frac{2h}{R}}\right) \quad (3)$$

First, the PMTs sensitivity was set by adjusting voltages on the PDU in a plateauing process (see **Appendix D**). Next, the GPS unit's firmware was updated (see **Appendix E**).

As mentioned before, the DAQ board executes onboard logic to determine whether PMT firings indicated an event. At the time of the experiment, plate 2 was found to be faulty. Therefore, we used only channels 0, 1, and 3 (corresponding to plates 0, 1, and 3), and we set the coincidence level to 3. This means that the DAQ board would register an event when plates 0, 1, and 3 were determined to have fired within the same timeframe.

The coincidence timeframe was determined by the gate width and pipeline delay parameters, configurable from the EQUIP application. For this experiment, gate width was set to 300 nanoseconds and pipeline delay was set to 100 nanoseconds. This is an optimal setting for recording muons due to the characteristics of the hardware. The magnitude of the PMT dark noise rate is ~1000 min^{-1}, which is an average spacing of 60 ms. As this is about 5 orders of magnitude longer than the gate width time, the impact of dark noise on the coincidence data could be safely ignored.

The detector was oriented parallel to the magnetic poles, for reasons previously discussed. Magnetic north was found based on the World Magnetic Model. Then, a map was used to find the direction of geographic north. A protractor was used

to find the direction of magnetic north relative to geographic north, and a piece of cardboard was positioned parallel to magnetic north. This provided a baseline for alignment of the detector itself. Additionally, data was collected at night, due to reasons previously discussed.

For reasons previously discussed, the detection of muons by the CRMD was modelled by a Poisson distribution, which has standard deviation as the square root of the mean. Thus, the relative standard uncertainty on the Poisson distribution was $N^{-\frac{1}{2}}$, where N is the number of events. Each angle was collected for at least 2,500 events to place an upper bound of 2% on the Poisson uncertainty. Data collection from each angle ranged from 7 minutes at 0° to about an hour at angles approaching 90°.

Data Processing

EQUIP has an option to report coincidence counts and reset the counter every 5 minutes. See **Appendix F** for the commands used. We calculated relative muon flux, using unit time as a minute, by averaging the coincidences for a given angle and dividing by five.

### Data Analysis
Relative muon flux and linear interpolation

We plotted relative muon flux on a scatter plot with smooth lines with respect to angle. Then, we linearly interpolated to find the approximate value of flux on angles that are a multiple of five. We later used this interpolated data in the regression step (**Figure 7**).

Convolution and regression

The sensitivity function was convolved with the relative muon angular-density function, setting $A = 1$ and $\alpha = 1000$ as an initial baseline for numerical analysis.
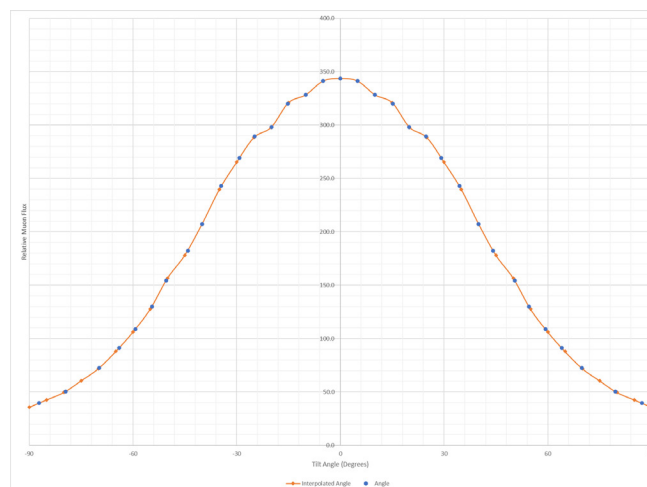
Figure 7. Relative muon flux and linear interpolation vs. tilt angle (degrees). Relative muon flux was linearly interpolated to multiples of 5° from the collected data.
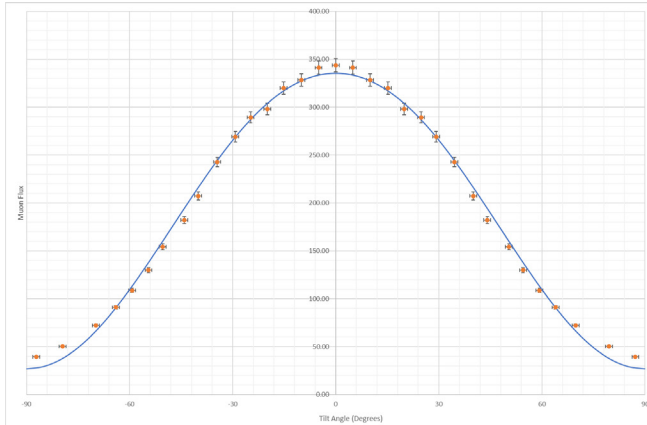
Figure 8. Comparison of relative muon flux and regressed convolution vs. tilt angle (degrees). The convolution was the function produced by the model, and the coincidence was observed data points with error bars. This series was used for least-squares regression to get parameters A and α.

We use the general attenuation form, $I \propto Ae^{-d/k} = Ae^{-\alpha(-\cos\theta + (\cos 2\theta + (h/R)^2 + 2h/R)^{1/2})}$, as previously derived. Holding α constant, a least-squares regression was done with A to get a definite answer in terms of α. Since A is multiplied linearly in the convolution expression, the regression can be written $UC[A] = CO$, where $UC = [UC_1\ UC_2\ \dots\ UC_N]$ and $CO = [CO_1\ CO_2\ \dots\ CO_N]$. These arrays are the unscaled convolutions (with $A = 1$) and interpolated coincidences for each of the measured angles. Then, using a standard regression result, $[A] = (UC^T UC)^{-1} UC^T CO$. Setting the parameter A to this expression in the spreadsheet made it dependent on α. Another parameter was calculated: the sum of the squares of the residues between the convolution and coincidence for each tilt angle. By manually adjusting α and minimizing this parameter, we accomplished least squares regression of the relative muon angular-density function (**Figure 8**).
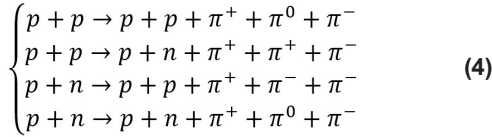
REFERENCES

1. "Cosmic rays." *NASA Goddard Space Flight Center*, web.archive.org/web/20121028154200/imagine.gsfc. nasa.gov/docs/science/know_l1/cosmic_rays.html.
2. Icecube Collaboration. "IceCube neutrinos point to long-sought cosmic ray accelerator." *IceCube South Pole Neutrino Observatory*, University of Wisconsin-Madison, 12 July 2018, icecube.wisc.edu/news/view/586.
3. Walker, John. "The Oh-My-God particle." *Fourmilab*, 4 Jan. 1994, www.fourmilab.ch/documents/ OhMyGodParticle/.
4. Nave, Carl R. "Cosmic rays." *HyperPhysics*, hyperphysics.phy-astr.gsu.edu/hbase/Astro/cosmic.html.
5. Tanabashi, M. *et al*. (Particle Data Group). "Review of Particle Physics." *Phys. Rev. D*, vol. 98, no. 3, 1 Aug. 2018, pp. 424-32, doi:10.1103/PhysRevD.98.030001.
6. "Lepton." *Encyclopaedia Britannica*, 2009, www. britannica.com/science/lepton. Accessed 9 Sept. 2019.
7. Nagamine, Kanetada. *Introductory Muon Science*. Cambridge University Press, 2003, p. 184.
8. CERN. "The standard model." *CERN*, 2013, home.cern/ science/physics/standard-model.
9. Ding, Chunyang. *Cosmic Ray Muons TeXtbook*. 2015, pp. 1-56.
10. Rylander, Jeff, *et al*. *QuarkNet cosmic ray muon detector user's manual series "6000" DAQ*. 1.1th ed., FermiLab QuarkNet, 2010, pp. i-53, quarknet.org/sites/default/files/ cf_6000crmdusermanual-small.pdf.
11. Mitra, Mausumi S., *et al*. "Empirical expressions for angular deviation of muons transmitted through slabs of iron, lead and uranium." *Nuclear Instruments and Methods in Physics Research Section A: Accelerators, Spectrometers, Detectors and Associated Equipment*, vol. 604, no. 3, 11 June 2009, pp. 684-93, doi:10.1016/j. nima.2009.02.037.
12. Braucher, R, *et al*. "In situ produced 10Be measurements at great depths: implications for production rates by fast muons." *Earth and Planetary Science Letters*, vol. 211, no. 3-4, 30 June 2003, pp. 251-58, doi:10.1016/S0012-821X(03)00205-X.

APPENDIX A
Muon generation and decay

The primary constituent of cosmic rays are high-energy protons. When these protons impact the Earth's upper atmosphere, they undergo nuclear reactions with atmospheric molecules, creating showers of particles including muons and pions (mesons composed of up/down quarks/antiquarks). Common reaction pathways include (10):

$$\begin{cases} p + p \rightarrow p + p + \pi^+ + \pi^0 + \pi^- \\ p + p \rightarrow p + n + \pi^+ + \pi^+ + \pi^- \\ p + n \rightarrow p + p + \pi^+ + \pi^- + \pi^- \\ p + n \rightarrow p + n + \pi^+ + \pi^0 + \pi^- \end{cases} \quad (4)$$

Furthermore, both muons and pions can be found in further decay processes of unstable particles generated by prior nuclear reactions. Charged pions then decay with a branching fraction of 0.9999 fairly quickly into muons and muon neutrinos (10):

$$\begin{cases} \pi^+ \rightarrow \mu^+ + \nu_\mu \\ \pi^- \rightarrow \mu^- + \overline{\nu_\mu} \end{cases} \quad (5)$$
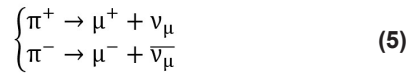
Cosmic ray muons typically have a relativistic factor of $\gamma = (4GeV)/(mc^2) + 1 \approx 39$. Travelling at *0.9997c*, muons take at least $\tau = 9km/0.9997c \approx 30\mu s$ to travel the roughly 9 km from where they are produced to the Earth's surface (14). Relativistic time dilation explains how muons can reach as far as the Earth's crust even though they have a mean lifetime of 2μs, since in the lab frame, they will have a mean lifetime of $\tau' = \gamma\tau \approx 79\mu s$. However, the proximity of these values means that a significant proportion of muons will decay before they reach the Earth's surface. The proportion that survives is given by $e^{-t/\tau'} \approx 70\%$, meaning that as many as 30% have decayed. This decay contributes a factor to the overall muon attenuation observation.

APPENDIX B
Data Tables

Table 1. Raw data on muonic flux vs. angle.

Angle (Degrees)	Channel 0 (min⁻¹)	Channel 1 (min⁻¹)	Channel 2 (min⁻¹)	Coincidence (min⁻¹)	Relative Uncertainty
87.2	1273.5	1130.7	1424.5	39.6	1.6300%
79.5	1363.3	1213.7	1514.6	50.3	0.9972%
69.8	1243.2	1225.1	1483.3	72.3	1.3147%
64.0	1332.8	1347.5	1531.4	91.2	1.9121%
59.3	1431.3	1406.4	1585.9	108.8	1.6205%
54.5	1418.8	1397.1	1589.4	130.0	1.9615%
50.4	1431.0	1354.2	1631.9	154.3	1.6100%
44.1	1485.9	1461.1	1642.3	182.1	1.9132%
40.0	1520.0	1543.1	1661.7	207.4	1.3888%
34.5	1574.2	1671.3	1703.7	243.0	1.4346%
29.2	1586.4	1671.6	1733.8	269.2	1.9274%
24.8	1248.1	1553.2	1704.5	289.3	1.5179%
19.9	1539.4	1530.0	1755.4	298.2	1.8312%
15.2	1567.6	1547.6	1758.5	320.0	0.8838%
10.0	1598.8	1582.5	1767.3	328.4	1.0075%
5.0	1617.8	1621.8	1765.7	341.3	0.8559%
0.0	1652.7	1646.6	1776.8	343.8	0.9117%

Note: Relative uncertainty on coincidence count was calculated by assuming a Poisson distribution for the coincidence with N = 2500. Channels 0, 1 had 1260 min⁻¹ dark noise, while channel 2 had 1445 min⁻¹ dark noise based on a least-squares fit $c_i \sim c + n_i$, which assumed dark noise rate was independent of detector angle and coincidence.

Table 2. Various fitted, calculated, and constant parameters.

Parameter	Value
A	1522 km
α	1015
h/R	0.00141
Sum of Squares	2108 min⁻²
λ	6.3 km

Note: A and α were used as they are in f(θ), h/R was the ratio of muon creation height to Earth's radius, and λ was the attenuation length of muons in Earth's atmosphere.

APPENDIX C
Average Muon Survivability

Let a spherical coordinate system be defined with the center of the Earth as the origin. Consider the point on the Earth's surface with polar angle $\theta = 0$ and the muons going toward that point. The range of muons possibly reaching that point can be seen as a portion of the outer sphere (**Figure 2**). This is a range of the polar angle from $0 \leq cos^{-1}R/(R + h) \leq \theta_{max}$. The distance from a point on the upper atmosphere with polar angle to the point on the Earth's surface is $d(\theta) = (2R(R + h)(1 - cos\ \theta) + h2)^{1/2}$. Assuming the number of incoming muons is proportional to surface area $dA = 2\pi(R + h) sin\ \theta\ d\theta$, the muon survivability can be shown to be:

$$\frac{\int_{-2\pi(R+h)}^{-2\pi R} \exp\left(-\frac{d(\theta)}{\lambda}\right) dA}{\int_{-2\pi(R+h)}^{-2\pi R} dA} = \frac{\int_0^{\cos^{-1}\frac{R}{R+h}} \exp\left(-\frac{\sqrt{2R(R+h)(1-\cos\theta)+h^2}}{\lambda}\right) 2\pi(R+h)\sin\theta\,d\theta}{\int_0^{\cos^{-1}\frac{R}{R+h}} 2\pi(R+h)\sin\theta\,d\theta} \quad (6)$$

This result can be evaluated numerically using constants outlined throughout the paper.

APPENDIX D
Plateau PMT sensitivity

To set up the DAQ for the plateauing process, set all the PDU dials to their minimum, corresponding to 0.300 V. Then, increase the voltage on plate 0 until the event count is between 40-60Hz. Set EQUIP to record the coincidence count for one minute between plates 0 and 1. After one minute, adjust the voltage on place 1 by a step size of 20 mV. Repeat until the voltage reaches 1 V. Graph the coincidence counts as a function of voltage, and look for a "plateau," or when *dy/dV* is at a minimum. This voltage is the optimal voltage for operation of plate 1. To finish plateauing all the plates, repeat these steps for plates 2 and 3, and then plateau plate 0 using plate 1 as a reference point.

APPENDIX E
Update GPS firmware

Use EQUIP to set the baud rate of the DAQ to 38400 by typing SB 123 2. Configure Tera Term to communicate with the serial port at the same baud rate. In Tera Term, put the DAQ into GPS download mode by typing UL 123. Disconnect the RJ45 cable and disconnect Tera Term.

Now short out JP5 on the GPS circuit board with a wire. Reconnect the RJ45 cable and run the update application on

the computer. Finally, reset the DAQ and verify the success of the update by checking the time and date by typing DG.

APPENDIX F
EQUIP settings

From EQUIP, a threefold coincidence was used with channels 0, 1, and 3. This was achieved with the terminal command "WC 00 2D".

The time register was set to 300 nanoseconds. This was achieved with the terminal commands "WT 01 00" and "WT 02 64".

The gate width was set to 100 nanoseconds. This was achieved with the terminal commands "WC 02 0A" and "WC 03 00".

Scalers were set to reset and record their values every 5 minutes. This was achieved with the terminal command "ST 3 5". The results will be printed every 5 minutes into a text file. Each time the result is printed, the file will show six space delimited items. The first is "DS", which signifies that the scalers are being displayed. Then follows four 32-bit words describing the scaler value on channels 0-3. The final 32-bit word is the coincidence rate in that five-minute interval.

APPENDIX G

Table 3. Table of abbreviations.

Abbreviation	Definition
CRMD	Cosmic Ray Muon Detector
DAQ	Data Acquisition
GPS	Global Positioning System
GUI	Graphical User Interface
HZE	High Atomic Number and Energy
PDU	Power Distribution Unit
PMT	Photomultiplier Tube